P H Y S I C A L   R E V I E W   L E T T E R S

ℭ

Optically Modulated Conduction in Chromophore-Functionalized Single-Wall Carbon Nanotubes

J. M. Simmons,[1] I. In,[2] V. E. Campbell,[2] T. J. Mark,[2] F. Léonard,[3] P. Gopalan,[2] and M. A. Eriksson[1]

[1]*Department of Physics, University of Wisconsin-Madison, Madison, Wisconsin 53706, USA*
[2]*Department of Materials Science and Engineering, University of Wisconsin-Madison, Madison, Wisconsin 53706, USA*
[3]*Sandia National Laboratories, Livermore, California 94551, USA*

We demonstrate an optically active nanotube-hybrid material by functionalizing single-wall nanotubes with an azo-based chromophore. Upon UV illumination, the conjugated chromophore undergoes a *cis-trans* isomerization leading to a charge redistribution near the nanotube. This charge redistribution changes the local electrostatic environment, shifting the threshold voltage and increasing the conductivity of the nanotube transistor. For a ~1%–2% coverage, we measure a shift in the threshold voltage of up to 1.2 V. Further, the conductance change is reversible and repeatable over long periods of time, indicating that the chromophore-functionalized nanotubes are useful for integrated nanophotodetectors.

Recent experiments demonstrating the use of individual single-wall carbon nanotube transistors as both photoabsorbers [1–3] and emitters [4,5] have enhanced the prospects for using nanotubes in optoelectronic devices. In the case of photoabsorbers, the ability to tune the absorption window is limited by difficulties in synthetically controlling the nanotube chirality, and thus the band structure, as well as the formation of bound excitons [6,7]. In principle these problems can be overcome by using chromophore-functionalized nanotubes [8–10], where the molecular photoabsorption can be synthetically tuned independent of the nanotube electronic structure. However, there are several issues that need to be addressed to make this approach viable: interactions between the chromophore and the nanotube may lead to scattering of the charge carriers and device degradation; in the case of photoswitching by charge transfer between the chromophore and the nanotube, the hybrid must have the correct band alignment between the molecular orbitals and the nanotube electronic states; photobleaching mechanisms in many chromophore systems can lead to the loss of optical activity.

To circumvent these issues, we demonstrate an approach based on the use of photoisomerization of organic chromophores to optically modulate the conduction in individual nanotube transistors. Chromophore isomerization causes a significant change in the molecular dipole moment, effecting a change in the local electrostatic environment. Atomistic modeling of the nanotube transistor in the presence of dipoles is used to support this mechanism. These optically active nanotube hybrids show no indication of bleaching and can be reliably switched over long periods of time. In contrast to a charge-transfer effect, the dipolar switching mechanism does not rely on the specific electronic states of the nanotube channel; thus this mechanism is general and can be applied to other semiconducting nanomaterial systems. In addition, synthetic control of the chromophore offers the ability to tune both the absorp-

tion wavelength and sensitivity of the nanotube-hybrid transistor.

We use an azobenzene-based chromophore, Disperse Red 1 (DR1), as the photoswitching sidewall functionality. This molecule is known to isomerize under UV illumination, accompanied by a significant change in the dipole moment [11]. Experiments have shown that at equilibrium, the DR1 chromophore is in the *trans* conformational state (Fig. 1) in which there is significant orbital overlap between the phenyl rings. Because of this conjugation and the presence of the strongly electronegative nitro end group, the *trans* conformation has a considerable, ~9 D, dipole moment [11]. Under UV light, the chromophore isomerizes to the *cis* conformation (Fig. 1) where the orbital overlap is significantly reduced, leading to a smaller,
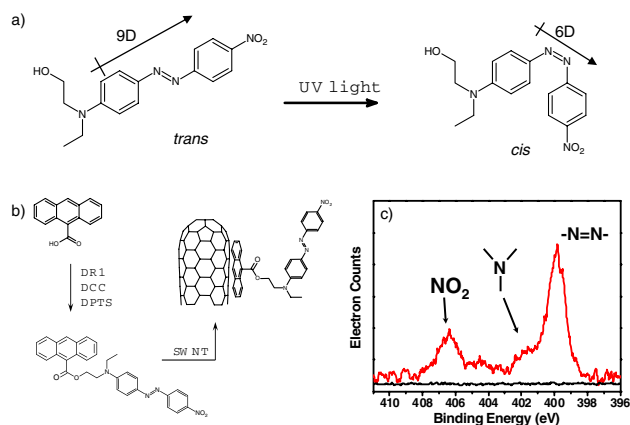

FIG. 1 (color online). (a) Under UV light, DR1 isomerizes from the equilibrium *trans* conformation to the metastable *cis* conformation. In doing so, the molecular dipole moment changes from 9 to 6 D. (b) Reaction scheme for noncovalent nanotube functionalization. [DPTS =4-(dimethylamino)-pyridinium *p*-toluenesulfonate] (c) N(1*s*) core level photoelectron spectrum of the physisorbed anthracene-DR1 functionality.

086802-1

~6 D, dipole moment. If left in ambient conditions, the *cis* isomer will relax to the more stable and less sterically hindered *trans* conformation.

We functionalize nanotubes using noncovalent attachment of the DR1 chromophore via an anthracene tether. Though such chromophores can be attached to the nanotube sidewalls either covalently or noncovalently, noncovalent attachment is advantageous because it only weakly perturbs the nanotube electronic states. Polycyclic aromatic hydrocarbons such as pyrene and anthracene have been shown to physisorb onto nanotubes by forming π-π bonds to the nanotube sidewall with little charge transfer [12,13]. Since most π-π bound molecules can be easily removed using common solvents, noncovalent attachment also offers the ability to reversibly functionalize nanotubes. The anthracene modified DR1 is synthesized from 9-anthracenecarboxylic acid and DR1 using a dicyclohexylcarbodiimide (DCC) esterification reaction (Fig. 1). The crude product is purified by silica gel chromatography and the structure is confirmed using ^{1}H-NMR [14]. After purification, the anthracene-DR1 is dissolved in dimethylformamide for application to the nanotubes. Pure anthracenecarboxylic acid is also dissolved for use as a nonfunctional control.

The individual nanotube transistors are fabricated on highly doped silicon wafers with a 500 nm thermal oxide using chemical vapor deposition (CVD) and subsequent lithography. The nanotubes are grown using iron and molybdenum nanoparticle catalysts at 900 °C using methane feedstock with hydrogen coflow [15]. Under these CVD conditions, the average nanotube diameter is ~1.6 nm. After growth, electron and atomic force microscopy are used to locate individual nanotubes and electron beam lithography, metal deposition, and 400 °C forming gas anneal (4:1 Ar/H_2) are used to form contacts. A total of 12 devices are processed for this study, nine of which functioned as transistors after fabrication.

After annealing, a drop of the anthracene-DR1 (or anthracenecarboxylic acid) solution is placed onto the chip and the sample is washed to remove the nonspecifically bound chromophores. X-ray photoelectron spectroscopy [XPS, Fig. 1(c)] measurements confirm that the chromophore remains after washing and yield a coverage of 1–2 molecules per 100 nanotube carbon atoms, calculated from the N(1s) to C(1s) intensity ratio [16]. I-V_g characteristics of individual single-wall carbon nanotube transistors before and after adsorption of the chromophore show minimal changes in the drain current, indicating that the anthracene-DR1 molecules cause minimal scattering of the charge carriers, and no degradation in device performance. Devices can exhibit threshold voltage shifts due to small chirality-dependent charge transfer from anthracene [13]. Gate voltage scans to high positive voltages show no indication of the *n*-channel opening up, indicating that the transistors are unipolar.

UV-induced switching is performed using a handheld UV lamp with 254 and 365 nm lines and a low intensity of

~100 μW/cm^2. Electrical measurements are performed in a nitrogen purged cell to eliminate the potential for ozone oxidation from UV excitation of the atmospheric oxygen [17]. While measuring the drain current through a nanotube transistor, the gate voltage is varied to acquire a series of I-V_g characteristics (Fig. 2). Before illumination with UV light, the transistor shows *p*-type behavior with a threshold voltage of ~1 V. When the chromophore is isomerized to the *cis* conformation, the threshold voltage is shifted to the right, in this case by 0.7 V, and does not depend on the wavelength of UV light used. The threshold voltage shift under illumination was measured for five nanotube transistors; all show positive threshold shifts with a range of 0.6–1.2 V. This shift could indicate a charge-transfer mechanism [9] or a change in the local electrostatic environment [18,19]. Charge transfer from the chromophore to the nanotube is inhibited by the alkane spacer and anthracene tether separating the chromophore and the nanotube and control experiments show no threshold voltage shift, indicating that there is no photoinduced charge transfer from the anthracene tether. An estimate of the amount of charge transfer needed for a 1 V threshold voltage shift gives $0.07e$/molecule, so we cannot entirely rule out charge transfer. However, since the UV photoisomerization and concurrent dipole moment change of DR1 is well established, we propose that the dipole moment change acts as a small local negative gate voltage. The large transistor threshold voltage swing is due to the relatively short spacer group used to separate the chromophore from the nanotube (~1 nm for anthracene-DR1).

To further test this mechanism, we performed quantum transport calculations of the nanotube transistor characteristics in the presence of dipoles. In brief, we use the nonequilibrium Green's function formalism implemented in a tight-binding formalism in conjunction with a Poisson solver to self-consistently calculate the charge and the electrostatic potential in the device, and the conductance
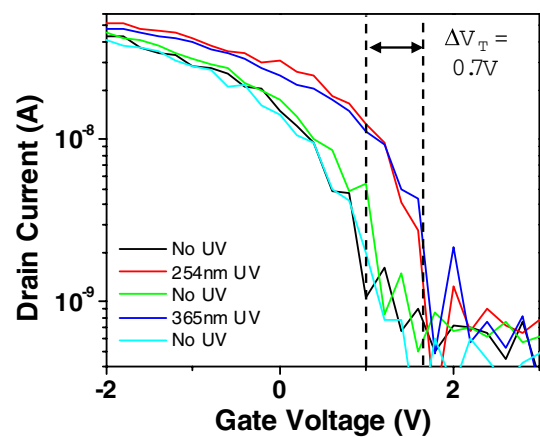

FIG. 2 (color online). Transistor characteristics showing threshold voltage shifts under UV light. The threshold voltage is shifted to the right by 0.7 V for both 254 and 365 nm light and is fully reversible.

[20,21] (this method is applicable to calculations of steady-state quantities; the time dependence of the switching, as discussed below, is beyond the scope of this approach). A schematic of the simulated device is shown in Fig. 3; it consists of a (17,0) nanotube (band gap 0.55 eV, radius 0.66 nm) sitting on SiO_2. At the ends of the computational cell, the nanotube is sandwiched between two metallic plates, forming the source and drain contacts. The bottom and top metallic plates have thicknesses of 2.25 and 2 nm, respectively, and are separated from the nanotube by 0.3 nm. The metal work function is 1 eV below the nanotube midgap, and after self-consistency, sits slightly below the valence band edge, creating an Ohmic contact. Because of the computational demands of the calculations, we cannot simulate the actual experimental device, instead, we focus on a smaller device of 35 nm channel length and with a gate oxide thickness of 4.5 nm. The results of our computations are then related to the experimental device by scaling the gate voltage by the ratio of the capacitances of the experimental and simulated device, using the expression for the capacitance $2\pi\varepsilon/\ln(2t/R)$, where t is the gate oxide thickness and R is the nanotube radius. Because of the high density of molecules on the nanotube surface, we assume that the dipole moment is perpendicular to the nanotube surface, and is modeled by a positive (negative) point charge of magnitude equal to the electron charge and at distance h ($h+d$) above the nanotube. From the molecule configuration we estimate $h = 1$ nm, and use a three-dimensional Gaussian distribution of the charge. The dipoles are evenly distributed on the nanotube using the range of experimentally measured chromophore densities. The *trans* to *cis* isomerization is studied by changing the value of d from 0.1 to 0.067 nm, reproducing the molecular dipole moments of 9 and 6 D.

The calculated conductance as a function of gate voltage is shown in Fig. 3 for the *trans* and *cis* cases, overlaid on the experimental data. A dipole spacing of 0.35 nm is used, corresponding to the midpoint of the range of chromophore densities measured by XPS. (The calculated conductance was rescaled by a factor $1/140$ to match the experimental conductance in the ON state of the nanotube transistor. The lower conductance of the experimental devices may be due to scattering in the nanotube or the presence of a small Schottky barrier at the contacts. The numerical results were also shifted by 0.65 V to match the threshold voltage of the *trans* experimental data. The need for this shift may be due to doping of the nanotube. The rescaling of the conductance and shift of the gate voltage are only necessary to reproduce the conductance curve prior to illumination. Once this is obtained, no further adjustment is made, and the shifted conductance curve is obtained by changing only the dipole moment.) A threshold voltage shift of 700 mV is found, in excellent agreement with the experiments and supporting the dipole change mechanism as the reason for the modulation of the nanotube conductance. Calculations were performed for several dipole densities. From these results, the uncertainty in the measured dipole density yields a range in the predicted threshold shift of approximately 0.45–0.95 V, correlating well with the 0.6–1.2 V shifts measured for other devices.

We turn next to the kinetics of the switching event, shown in Fig. 4. In (a), *trans* to *cis* isomerization under 254 nm UV light leads to a uniform increase in the drain current. In addition, the magnitude of the current change is dependent on the gate voltage, with the largest signal arising from the subthreshold region of the I-V_g characteristic near $V_g = 0$ V (see Fig. 2). In both cases shown, the sample was illuminated 3 times, each of which led to an appreciable increase in the measured drain current. All fabricated transistors show increased drain current under UV illumination, with abrupt and repeatable transitions. The transistors have shown repeatable switching for more than 100 cycles and over several months.

DR1 has a finite absorption window in the UV region such that most UV wavelengths will isomerize the chromophore. Specifically, DR1 is sensitive to both 254 and 365 nm UV light, with an approximate 5:1 absorbance ratio (254 nm : 365 nm). Indeed, we see in Fig. 4(b) that 365 nm UV light also leads to modulation of the nanotube conduction, though the magnitude of change is the same for both wavelengths. Given the 5:1 absorbance contrast, the equal modulation for both UV wavelengths indicates that the isomerization has saturated under the low intensity UV lamp. Though the current in this sample decreases under continued 365 nm illumination, implying a relaxation of some chromophores to the *trans* state, other samples do not show this decrease and is thus specific to this device.
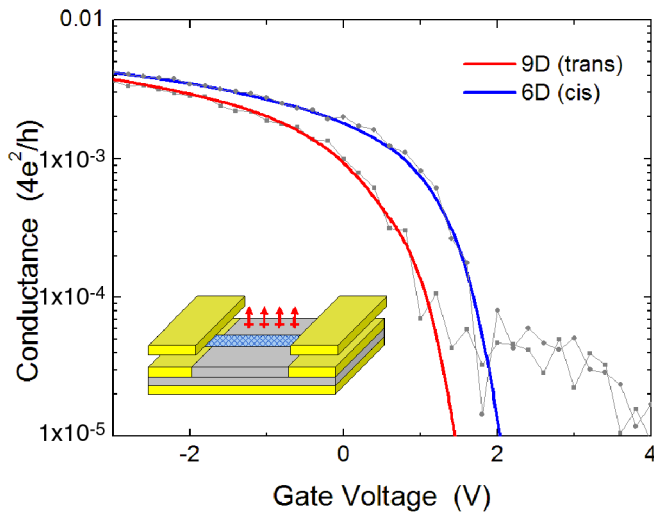

FIG. 3 (color online). Device simulations of the nanotube conductivity for both chromophore isomers (solid lines) compared with the experimental data (gray symbols). The transistor characteristic for the 9 D *trans* isomer (red curve, left) shifts toward positive gate voltages when the chromophore switches to the 6 D *cis* isomer (blue curve, right). As seen in the experiments, the threshold voltage is shifted to the right by 700 mV. Inset: Sketch of nanotube transistor used in the simulations, with the red arrows indicating the molecular dipoles.
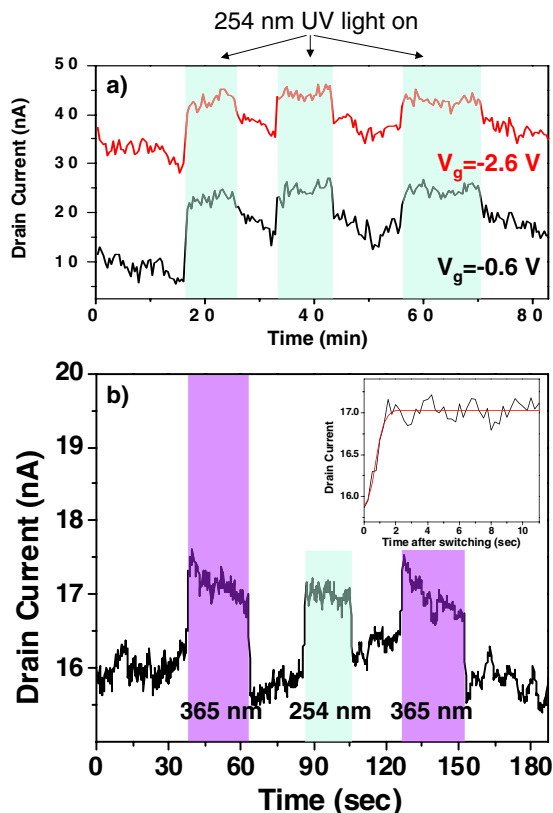
FIG. 4 (color online).   Time traces at fixed gate voltage for two different nanotube-hybrid transistors showing multiple repeatable switching events under both 254 and 365 nm light. Lower inset: Close up view of the transition under 254 nm light from the bottom graph. The smooth red line is a fit to the data using the Avrami equation (see text) with a time constant of ~2 s.

The inset to Fig. 4(b) shows a close-up view of the transition region under 254 nm UV light. The line through the data is a fit using the Avrami equation, $\Delta I = 1 - e^{-Kt^n}$, where $n = 2$ [22]. Using the time it takes for the current to change from 10% to 90% of the full signal, we can extract a rise time of ~2 s. The off-time is approximately the same, as are the switching times for 365 nm light. This rise time seems surprisingly long for a molecular switching event, but is consistent with solid state implementations of DR1 in polymer matrices where molecule-molecule interactions can inhibit the kinetics of the isomerization [23]. Because the chromophores form a dense layer on the nanotube side walls, steric interactions between chromophore units could reduce the overall switching rates. Indeed, the $n = 2$ Avrami exponent is characteristic of a 2D growth mechanism from randomly dispersed nuclei, suggesting that the isomerization proceeds from a few *cis* conformers in the DR1 layer. The measured switching time is also as fast or faster than other chromophore-nanotube systems. Experiments using other chromophore systems show switching times on the order of tens to thousands of seconds [8–10]. Assuming that sterics dominate the transition rate, diluting the chromophore concentration on the nanotube side wall could accelerate the switching.

In summary, we have demonstrated the ability to noncovalently functionalize individual nanotube transistors using an azobenzene dye. When the chromophore photoisomerizes, the resulting change in dipole moment modifies the local electrostatic potential and modulates the transistor conductance by shifting the threshold voltage. The functionalized transistors show repeatable switching for many cycles and a modest ~2 s switching time. The low (~100 μW/cm^2) intensities necessary to optically modulate the transistor are in stark contrast to measurements of intrinsic nanotube photoconductivity which typically require 1 kW/cm^2 intensities [2]. In addition, synthetic control of the nanotube-hybrid systems should allow the tuning of the absorption window and magnitude of dipole switching.

[1] K. Balasubramanian *et al.*, Nano Lett. **5**, 507 (2005).
[2] M. Freitag *et al.*, Nano Lett. **3**, 1067 (2003).
[3] Y. Ohno *et al.*, Jpn. J. Appl. Phys. **44**, 1592 (2005).
[4] J. Chen *et al.*, Science **310**, 1171 (2005).
[5] J. A. Misewich *et al.*, Science **300**, 783 (2003).
[6] C. L. Kane *et al.*, Phys. Rev. Lett. **90**, 207401 (2003).
[7] F. Wang *et al.*, Science **308**, 838 (2005).
[8] X. Guo *et al.*, J. Am. Chem. Soc. **127**, 15 045 (2005).
[9] D. S. Hecht *et al.*, Nano Lett. **6**, 2031 (2006).
[10] L. Valentini *et al.*, J. Appl. Phys. **99**, 114305 (2006).
[11] Y. Atassi *et al.*, Pure Appl. Chem. **70**, 2157 (1998).
[12] R. J. Chen *et al.*, J. Am. Chem. Soc. **123**, 3838 (2001).
[13] J. Lu *et al.*, J. Am. Chem. Soc. **128**, 5114 (2006).
[14] ^{1}H-NMR: 300 MHz, CDCl3, TMS 1.11 (d,3H), 3.29 (q, 2H), 3.51 (t, 2H), 4.33 (t, 2H), 7.01-8.49 (m, 17H).
[15] J. Kong *et al.*, Chem. Phys. Lett. **292**, 567 (1998).
[16] J. F. Moulder *et al.*, *Handbook of X-Ray Photoelectron Spectroscopy* (Perkin-Elmer, Eden Prairie, MN, 1992).
[17] J. M. Simmons *et al.*, J. Phys. Chem. B **110**, 7113 (2006).
[18] M. S. Marcus *et al.*, J. Appl. Phys. **100**, 084306 (2006).
[19] L. Larrimore *et al.*, Nano Lett. **6**, 1329 (2006).
[20] F. Léonard, Nanotechnology **17**, 2381 (2006).
[21] F. Léonard *et al.*, Nanotechnology **17**, 4699 (2006).
[22] M. Avrami, J. Chem. Phys. **7**, 1103 (1939).
[23] R. Loucif-Saïbi *et al.*, Chem. Mater. **5**, 229 (1993).